# Theory of autoionization of Xe under two- and three-photon excitation

P. Gangopadhyay, X. Tang, P. Lambropoulos,* and Robin Shakeshaft
*Department of Physics, University of Southern California, Los Angeles, California 90089-0484*
(Received 27 December 1985)

We present calculations of two- and three-photon ionization of Xe in the energy region between and slightly above the two ionization thresholds. The resonance structure between the thresholds is treated by multichannel quantum-defect theory and the summation over intermediate states by truncating the sum. Predictions for resonance profiles and photoelectron angular distributions are also presented.

## I. INTRODUCTION

Although the rare gases and especially Xe have, for several years now, been serving as a testing ground for experimental multiphoton ionization studies, relevant calculations[1,2] have been very scarce. The complexity of these atoms is, of course, the main reason for the scarcity of such calculations. The problem cannot, however, be avoided forever and it is our belief that one must make some attempts even if they have to be not very accurate at first. Two types of experiments during the last three or four years make this unattractive task even more imperative. One has to do with above-threshold ionization[3–5] or continuous-continuous transitions in which the electron keeps absorbing photons even after having absorbed the minimum number of photons necessary to cross the threshold. These are observations with either 1064-nm or 532-nm radiation and intensities around $10^{13}$ W/cm$^2$. The other type of experiments deal with multiphoton, multiple ionization under much higher intensity ($10^{14}$–$10^{16}$ W/cm$^2$) and shorter wavelengths (193 nm). Multiple ionization has also been observed[6,7] at $\lambda=1064$ nm and $\lambda=532$ nm. The atom of Xe has figured prominently in both types of experiments. For radiation of 193 nm, one electron is ejected from Xe by two-photon ionization and a second electron by a four-photon process. In fact the first (two-photon) process falls within the autoionizing region between the $P_{3/2}$ and $P_{1/2}$ thresholds. It is at this type of process that we are aiming at first with the undertaking of the calculations reported in this paper. The only other calculations in rare gases, except He, that we are aware of, are those of Pindzola and Kelly[1] dealing with many-body theory of two-photon ionization of Ar and of McGuire[2] dealing with two- and three-photon ionization of rare gases using a Green's function based on a single-electron model. To deal with the autoionizing region, however, we must include the channel couplings which causes the wave function to depart substantially from the single-electron model.

## II. BRIEF INTRODUCTION TO PERTURBATION THEORY

For multiphoton ionization, a generalized cross section (GCS) is defined through the relation

$$W^{(N)}=\hat{\sigma}^{(N)}F^N , \tag{1}$$

where $F$ is the photon flux density in number of photons/cm$^2$ sec, $W^{(N)}$ is the rate of the $N$-photon process, and $\hat{\sigma}^{(N)}$ is the generalized cross section in cm$^{2N}$sec$^{N-1}$. When the final state is in the continuum (ionization) the generalized cross section is given by[8]

$$\hat{\sigma}^{(N)}=\frac{(2\pi\alpha)^N}{4\pi^2}\frac{mk}{\hbar}\omega^N\int |M_{fg}^{(N)}(\Omega_k)|^2 d\Omega_k , \tag{2}$$

where the integration is over solid angles corresponding to all possible directions $\mathbf{k}$ of the ejected electron. In the expression above, $\alpha$ is the fine-structure constant, $k$ the magnitude of the wave vector of the ejected electron, $\hbar\omega=E_p$ the energy of the photon, and $N$ the order of the process. The transition amplitude $M_{fg}^{(N)}$ is given by

$$M_{fg}^{(N)}=\sum_{a_{N-1}}\sum_{a_2}\sum_{a_1}\frac{\langle f|\mathbf{r}\cdot\boldsymbol{\epsilon}|a_{N-1}\rangle\cdots\langle a_2|\mathbf{r}\cdot\boldsymbol{\epsilon}|a_1\rangle\langle a_1|\mathbf{r}\cdot\boldsymbol{\epsilon}|g\rangle}{[E_{a_{N-1}}-E_g-(N-1)E_p]\cdots(E_{a_2}-E_g-2E_p)(E_{a_1}-E_g-E_p)} , \tag{3}$$

where the $a_i$'s represent all possible intermediate states allowed by the selection rules and $\boldsymbol{\epsilon}$ is the unit polarization vector of the radiation mode. The calculation of the cross section is reduced to the calculation of the matrix element. The matrix element contains the details of the atomic structure, the wave function, and the energy levels of the atom.

As in any multiphoton calculation,[8] we need good wave functions and a method for performing the infinite summations over the intermediate states or equivalently the

 

Green's function. The latter is not practical to construct if the channel couplings are to be included. The approach we have chosen is multichannel quantum-defect theory (MQDT) especially in the form employed by Lu and Fano[9,10] in the analysis of photoabsorption in Xe. The summation over intermediate states is performed by truncating the sum to a finite number of terms. By employing MQDT, we can account for the channel couplings, thus obtaining relatively accurate matrix elements. Truncation is the price we pay which, however, is expected to be not too serious an approximation since none of the calculations we report fall within a deep minimum where the complete summation becomes essential. In any case, it is with trial and error that the level of accuracy is ultimately assessed in such complex calculations. The results of this paper were obtained by including 27 states for the two-photon process and 59 states for the three-photon process. Since in all cases, the frequency was below the first single-photon as well as two-photon excited states no interference minima were involved. As a result, the error due to truncation alone is not expected to be more than a factor of 2.

## III. MQDT: A BRIEF REVIEW

This is not the place to review MQDT in detail, summaries of which abound in the literature. For Xe, far from the ionic core, the excited electron channels are described by $j$-$j$ coupling. But these asymptotic channel states $|i\rangle$ are not eigenstates of the electron-ion system at small distances. In that region, close-coupling eigenchannels $|\alpha\rangle$ are defined which are appropriate to the short-range interaction. Two asymptotic channel states $|i\rangle$ and $|j\rangle$ are connected through the $|\alpha\rangle$ states and this connection is expressed through the scattering matrix $S_{ij}$ which can be written in terms of diagonal matrix elements $\exp(2i\pi\mu_\alpha)$ as

$$S_{ij}=\sum_\alpha U_{i\alpha}\exp(2i\pi\mu_\alpha)U^\dagger_{\alpha j}\ . \tag{4}$$

The $U_{i\alpha}$'s form the frame transformation matrix and the $\mu_\alpha$'s are the eigenphase shifts of the scattering eigenstates $|\alpha\rangle$. In a heavy atom-like Xe, where the spin-orbit interaction is strong, the main contribution to $U_{i\alpha}$ comes from the $(LS/jj)$ transformation coefficients. The spin-orbit interaction in Xe gives rise to two ionization thresholds $I_{3/2}$ and $I_{1/2}$ labeled by the $J$ of the residual ion which is either $P_{3/2}$ or $P_{1/2}$, respectively, with $I_{3/2}$ being energetically lower. In the MQDT formalism, the final state of the excited electron plus ion system can be written in terms of known functions, if the parameters $U_{i\alpha}$, $\mu_\alpha$, $I_{3/2}$, and $I_{1/2}$ are known. They can be determined from experimentally obtained spectroscopic data or, in principle, by *ab initio* calculations. In this paper, the parameters are obtained from experimental information through the Lu-Fano[9,10] plots or extrapolations thereof.

Two different expressions for the cross sections—one in the autoionizing region between the two thresholds and another in the open continuum above $I_{1/2}$—are necessary. They are discussed separately below.

### A. Open continuum

The energy region above 13.45 eV specifies the open continuum region as all channels are open. In the open region the electronic state is expanded in terms of the usual angular momentum partial waves as follows:

$$|f_{m_s m_{J_c}}(k;r)\rangle=4\pi\sum_{l,m_l} i^l e^{i\delta_l}Y_{lm_l}(\theta,\phi)\sum_{j_k,J}\langle lsj_k\,|\,m_l m_s m_{j_k}\rangle\langle J_c j_k J\,|\,m_{J_c} m_{j_k} M_J\rangle\,|\,J_c j_k J M_J\rangle \tag{5}$$

which disentangles the wave vector $\mathbf{k}(k,\theta,\phi)$ from the $\mathbf{r}$ dependence. The $r$ dependence is contained in $|J_c j_k J M_J\rangle$. $J_c$ is the total angular momentum of the core, $l$ and $s$ refer to the angular and spin quantum number of the electron, and $J$ is the total angular momentum of both electron and the ion core. The $m_l, m_s, m_{j_k}, M_J$ are projections of the respective angular momenta. The matrix element for an $N$-photon amplitude is given by

$$\begin{aligned}M^N(\theta,\phi)&=\langle f_{m_s m_{J_c}}(k;r)\,|\,r^{(N)}\,|\,g\rangle\\&=\sum_\alpha\langle f_{m_s m_{J_c}}(k;r)\,|\,\alpha\rangle\langle\alpha\,|\,r^{(N)}\,|\,g\rangle\\&=4\pi\sum_i\sum_\alpha\sum_{l,m_l} i^l e^{i\delta_l}Y_{lm_l}(\theta,\phi)\sum_{j_k,J}\langle lsj_k\,|\,m_l m_s m_{j_k}\rangle\langle J_c j_k J\,|\,m_{J_c} m_{j_k} M_J\rangle\sum_\alpha D^{(N)}_\alpha U^\dagger_{\alpha i}e^{-i\pi\mu_\alpha}\ ,\end{aligned} \tag{6}$$

where $D^{(N)}_\alpha=\langle\alpha\,|\,r^{(N)}\,|\,g\rangle$ is an $N$th-order radial dipole matrix element connecting the ground state with the channel states $|\alpha\rangle$ which obey $\langle\alpha\,|\,i\rangle=U^\dagger_{\alpha i}$. The phase factor $e^{-i\pi\mu_\alpha}$ is to be inserted so that the amplitude of the exponentially ly increasing wave vanishes in all closed channels. When the matrix element is squared the sum over $m_l$ is incoherent as $m_{J_c}$ and $m_s$ are not measured,

$$|M^{(N)}_{fg}(\theta)|^2=(4\pi)^2\sum_{m_l}\left|\sum_i\sum_l i^l e^{i\delta_l}Y_{lm_l}(\theta,\phi)\sum_{j_k J}\langle lsj_k\,|\,m_l m_s m_{j_k}\rangle\langle J_c j_k J\,|\,m_{J_c} m_{j_k} M_J\rangle\sum_\alpha D^{(N)}_\alpha U^\dagger_{\alpha i}e^{-i\pi\mu_\alpha}\right|^2\ . \tag{7}$$

In the open region, the expression for the total (angle-integrated) transition probability is given by

$$\int |M_{fg}^{(N)}(\theta)|^2 d\Omega_{\mathbf{k}} = (4\pi)^2 \sum_i \left| \sum_\alpha D_\alpha^{(N)} e^{-i\pi\mu_\alpha} U_{\alpha i}^\dagger \right|^2_{(J_c=3/2)} + (4\pi)^2 \sum_i \left| \sum_\alpha D_\alpha^{(N)} e^{-i\pi\mu_\alpha} U_{\alpha i}^\dagger \right|^2_{(J_c=1/2)} . \quad (8)$$

For $J=1$, for example, the index $i$ assumes the values 1,2,3,4,5 representing, respectively, the five channels $[^2P_{3/2}]d_{5/2}$, $[^2P_{3/2}]d_{3/2}$, $[^2P_{3/2}]s_{1/2}$, $[^2P_{1/2}]d_{3/2}$, and $[^2P_{1/2}]s_{1/2}$. Correspondingly, the index $\alpha$ of the close-coupling eigenfunctions $\Psi_\alpha$ runs from 1 to 5.

### B. Autoionizing region

For the expressions inside the autoionizing region (12.13 to 13.45 eV), we need a third set of channel states $\psi_\rho(r)$ which behave as open channels for large $r$ but have bound character for small $r$. The matrix element is given by

$$\begin{aligned} M_{fg}^{(N)}(\theta,\phi) &= \langle f_{m_s m_{J_c}}(k;r) \,|\, r^{(N)} \,|\, g \rangle \\ &= \sum_{\alpha,\rho} \langle f_{m_s m_{J_c}}(k;r) \,|\, \rho \rangle \langle \rho \,|\, \alpha \rangle \langle \alpha \,|\, r^{(N)} \,|\, g \rangle \\ &= 4\pi \sum_{\alpha,\rho} \sum_i \sum_{l,m_l} i^l e^{i\delta_l} Y_{lm_l}(\theta,\phi) \sum_{j_k,J} \langle l s j_k \,|\, m_l m_s m_{j_k} \rangle \langle J_c j_k J \,|\, m_{J_c} m_{g_k} M_j \rangle \frac{T_{i\rho}}{N_\rho} D_\alpha^{(N)} \frac{A_\alpha}{N_\rho} , \end{aligned} \quad (9)$$

where another set of transformation coefficients $\langle \rho \,|\, \alpha \rangle = (A_\alpha / N_\rho)$ has been introduced with $N_\rho$ being a normalization factor (containing most of the energy dependence). The coefficients $A_\alpha$ satisfy the relations

$$\sum_\alpha U_{i\alpha} \sin[\pi(\mu_\alpha - \tau_\rho)] A_\alpha = 0 \quad (10)$$

for all $i$ with $\pi\tau_\rho$ being the eigenphase shifts of the collision eigenfunction $\psi_\rho$. The total phase shift is $\delta_{\rho(l)} = \eta_l + \pi\tau_\rho$, where $\eta_l$ is the Coulomb phase shift of the $l$th partial wave. The coefficient $T_{i\rho} = \langle i \,|\, \rho \rangle$ represents the probability amplitude of the $i$th channel wave function in the state $\psi_\rho$. In the calculation of the total transition probability, the sums over $\rho$, $i$, $\alpha$, and partial waves $l$ contribute coherently. The final expression has the form

$$\int |M_{fg}^{(N)}(\theta)|^2 d\Omega_{\mathbf{k}} = (4\pi)^2 \sum_\rho \left| \sum_\alpha D_\alpha^{(N)} \frac{A_\alpha}{N_\rho} \right|^2 . \quad (11)$$

## IV. RESULTS AND DISCUSSION

A sample of results containing the main features of the processes are shown in Figs. 1—4 and Tables I and II. The first two figures summarize the structure of the two- and three-photon ionization GCS inside the autoionizing region. In both cases, the background is of a magnitude typical of the respective order, without the deep minima found in single-electron atoms. In three-photon ionization, for example, the deep minima can be as low as $10^{-83}$ $cm^6 sec^2$, while in Fig. 2, the background is about 6 orders of magnitude larger. The main reason for the absence of deep minima is the relatively large number of contributing channels whose interference smooths out the deep minima that would exist in a single channel.

The peaks represent autoionizing resonances corresponding to energies at which $\pi\tau_\rho$ changes by $\pi$. Each peak is characterized by the total angular momentum $J$. Only the $J=1$ peaks of Fig. 2 could have been observed in single-photon uv photoionization experiments. It appears that the $J=1$ peaks around 12.5 and 12.9 eV correspond to those observed by Heinzmann.[11] The line shape, however, is not identical to that observed by Heinzmann. There is no strict requirement for a $J=1$ autoionizing peak reached by a three-photon transition to have the same line shape it has in a single-photon transition. The two line shapes will in general be different even without taking into account laser intensity effects which cause distortions of a different nature.[12,13] Effects of this type are not included in Figs. 1 and 2 where all structure is due to the interatomic interactions themselves. All peaks of Fig. 1 and those with $J=3$ of Fig. 2 represent new predictions

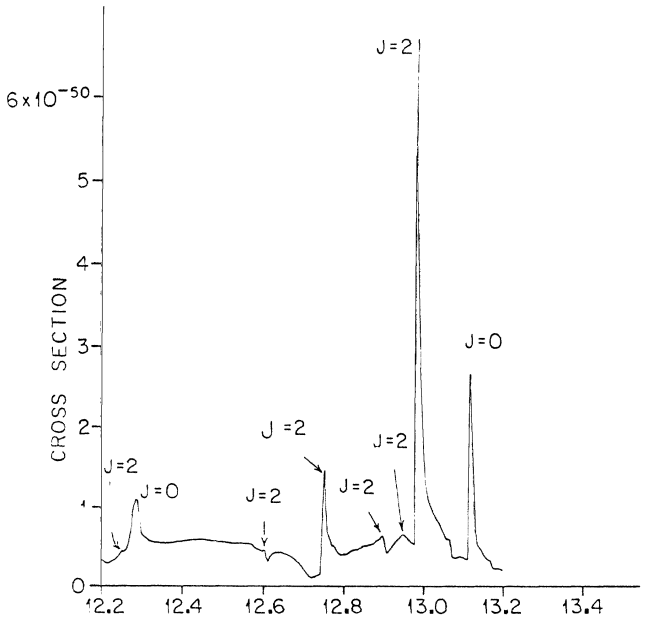


FIG. 1. Two-photon generalized cross section of Xe inside the autoionizing region in units of $cm^4$ sec.

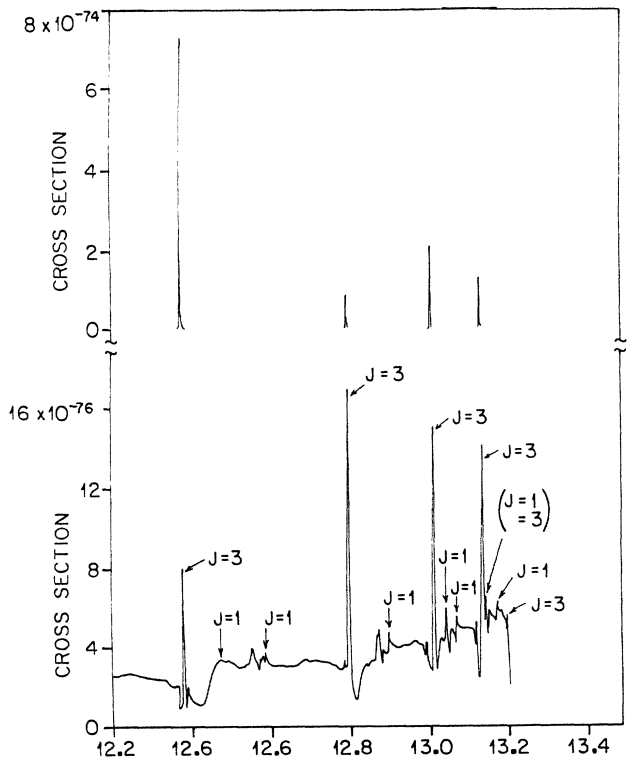


FIG. 2. Three-photon generalized cross section of Xe inside the autoionizing region in units of $cm^6 sec^2$.

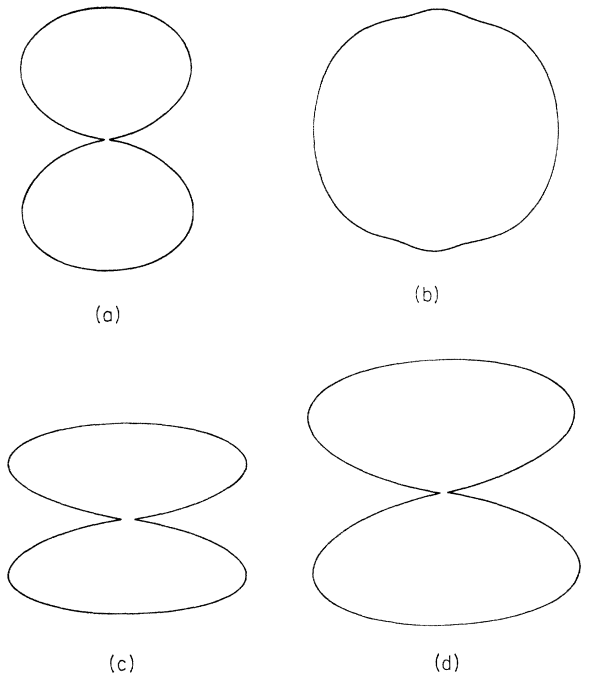


FIG. 4. Angular distribution of the outgoing electron with final electron energy above the $I_{1/2}$ threshold. (a) and (b) correspond to two-photon angular distributions with the residual core in $J_c=\frac{1}{2}$ and $J_c=\frac{3}{2}$, respectively ($E=16.86$ eV). (c) and (d) correspond to three-photon angular distributions with the residual core in $J_c=\frac{1}{2}$ and $J_c=\frac{3}{2}$, respectively ($E=14$ eV).

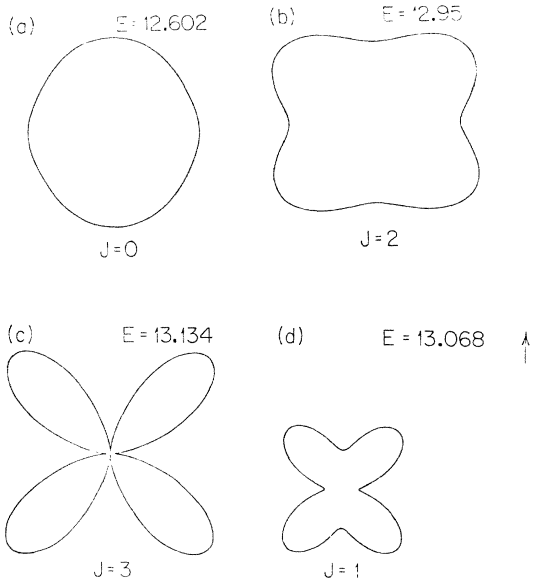


FIG. 3. Typical angular distributions of photoelectrons at autoionizing resonances. The energies $E$ represent the total energy above the ground state. (a) and (b) correspond to two-photon ionization while (c) and (d) correspond to three-photon ionization. The arrow indicates the direction of the photon polarization.

as they could not have been seen in single-photon transitions owing to the selection rules on $\Delta J$ and parity.

The GCS above the $I_{1/2}$ threshold is expected to have a smooth dependence on energy until a resonance with an intermediate bound state is reached. In Tables I and II we list representative values up to the point where the GCS begins to rise as it approaches the first such intermediate resonance in each case; the $6s$ ($J_c=\frac{1}{2}$) for two-photon and the $6p$ ($J_c=\frac{1}{2}$) for three-photon ionization. The values of our GCS compare well with those of McGuire[2] who has reported calculations only above the $I_{1/2}$ threshold. Ex-

TABLE I. Two-photon generalized cross sections of Xe in the open continuum.

| Total energy (eV) | Two-photon GCS with residual core in angular momentum state $J=\frac{3}{2}$ ($cm^4 sec$) | Two-photon GCS with core in $J=\frac{1}{2}$ ($cm^4 sec$) |
|---|---|---|
| 14 | $0.96\times10^{-50}$ | $1.02\times10^{-50}$ |
| 14.501 | $0.74\times10^{-50}$ | $0.8\times10^{-50}$ |
| 15.002 | $0.64\times10^{-50}$ | $0.74\times10^{-50}$ |
| 15.5 | $0.50\times10^{-50}$ | $0.88\times10^{-50}$ |
| 16.001 | $0.82\times10^{-50}$ | $1.54\times10^{-50}$ |
| 16.502 | $2.51\times10^{-50}$ | $6.71\times10^{-50}$ |
| 16.871 | $2.84\times10^{-46}$ | $9.34\times10^{-46}$ |

act agreement is not expected given the rather significant differences between the wave functions employed in the respective calculations.

A sensitive and important feature of any multiphoton ionization process is the photoelectron angular distribution. Although its experimental observation is more demanding, its input on the validity of theoretical calculations can be decisive. We show first four examples of photoelectron angular distributions corresponding to energies of selected autoionizing peaks (Fig. 3). Each of these distributions corresponds to a peak with different $J$. We find that the main features of the distributions are determined by the order of the process (as expected) and by $J$. In all of these examples, the distributions exhibit a rather unusual form which is not typical of distributions for the same order in other atoms. Thus the two-photon ionization distributions show an unusually large isotropic component while the three-photon distributions exhibit unusually large anisotropy. In all of these cases the ion is left in the $J=\frac{3}{2}$ state since we are between the two thresholds. The distributions do change significantly when the final electron energy is above the $I_{1/2}$ threshold as shown in Fig. 4. Their general shape is more typical although they still retain a rather unusual blend of anisotropy.

In summary, we have shown that two- and three-photon ionization of Xe between the first two ionization thresholds exhibits substantial structure with resonance peaks rising 2 and 3 orders of magnitude above the background. Similar structure is expected to exist in all rare gases except He. The background cross sections themselves are of relatively good size which suggests that ionization through that region should be relatively efficient. The even-parity structure should be present in four-photon ionization as well. In that case, however, additional structure would be expected due to states with $J=4$. But even for three-photon ionization, we cannot be sure that we have accounted for all the existing structure since the necessary spectroscopic information on $g$ states is rather incomplete. For two-photon ionization, on the other hand, the structure should be fairly complete, at least as far as a MQDT analysis allows. Given the large generalized cross sections in that region and the relatively high background, it is evident that, in recent experiments in Xe with radiation of wavelength $\lambda=193$ nm, the two-photon ejection of one electron was an extremely fast process. This implies that the transition $Xe+2\hbar\omega\rightarrow Xe^+$ occurs with probability equal to one well before the laser intensity can reach the value $10^{14}$ W/cm$^2$.

TABLE II. Three-photon generalized cross sections of Xe in the open continuum.

| Total energy (eV) | Three-photon GCS with core in $J=\frac{3}{2}$ (cm$^6$ sec$^2$) | Three-photon GCS with core in $J=\frac{1}{2}$ (cm$^6$ sec$^2$) |
|---|---|---|
| 14 | $2.02\times10^{-76}$ | $3.15\times10^{-76}$ |
| 14.11 | $2.97\times10^{-76}$ | $3.6\times10^{-76}$ |
| 14.21 | $4.51\times10^{-76}$ | $5.2\times10^{-76}$ |
| 14.31 | $7.59\times10^{-76}$ | $9.2\times10^{-76}$ |
| 14.41 | $1.56\times10^{-75}$ | $7.6\times10^{-75}$ |
| 14.506 | $3.282\times10^{-73}$ | $2.91\times10^{-72}$ |

It is conceivable that some of these resonances can serve as intermediate states for the absorption of more photons within the continuum. It is in addition expected that there will be excitation of one of the $5s^2$ electrons, since such an excitation corresponds to one of the low excited states of $Xe^+$. These and related questions are planned to be the topic of a follow-up publication.

## ACKNOWLEDGMENT

This work was supported by the National Science Foundation through Grant Nos. PHY-8119010 and PHY-8306263.

*Also at the Physics Department and the Research Center of Crete, University of Crete, Iraklion, Crete, Greece.

[1]M. S. Pindzola and H. P. Kelly, Phys. Rev. A **11**, 1543 (1975).
[2]E. J. McGuire, Phys. Rev. A **24**, 835 (1981).
[3]P. Agostini, M. Clement, F. Fabre, and G. Petite, J. Phys. B **14**, L491 (1981).
[4]P. Kruit, H. G. Muller, J. Kimman, and M. J. van der Wiel, J. Phys. B **16**, 937 (1983).
[5]R. Hippler, H. J. Humpert, H. Schwier, S. Jetzke, and H. O. Lutz, J. Phys. B **15**, L713 (1983).
[6]T. S. Luk, H. Pummer, K. Boyer, M. Shakidi, H. Egger, and C. K. Rhodes, Phys. Rev. Lett. **51**, 110 (1983).
[7]A. L'Huillier, L.-A. Lompre, G. Mainfray, and C. Manus, Phys. Rev. Lett. **48**, 1814 (1982); Phys. Rev. A **27**, 2503 (1983).
[8]P. Lambropoulos, Adv. At. Mol. Phys. **12**, 87 (1976).
[9]K. T. Lu, Phys. Rev. A **4**, 579 (1971).
[10]K. T. Lu and U. Fano, Phys. Rev. A **2**, 81 (1970).
[11]U. Heinzmann, J. Phys. B **13**, 4353 (1980); **13**, 4367 (1980).
[12]Y. S. Kim and P. Lambropoulos, Phys. Rev. A **29**, 3159 (1984).
[13]P. Lambropoulos, Phys. Rev. Lett. **55**, 2141 (1985).